

# Selective Attention in an Insect Visual Neuron

Steven D. Wiederman<sup>1,\*</sup> and David C. O'Carroll<sup>1,\*</sup><sup>1</sup>Adelaide Centre for Neuroscience Research, School of Medical Sciences, The University of Adelaide, Adelaide, SA 5005, Australia

## Summary

Animals need attention to focus on one target amid alternative distracters. Dragonflies, for example, capture flies in swarms comprising prey and conspecifics [1], a feat that requires neurons to select one moving target from competing alternatives. Diverse evidence, from functional imaging and physiology to psychophysics, highlights the importance of such “competitive selection” in attention for vertebrates [2–5]. Analogous mechanisms have been proposed in artificial intelligence [6] and even in invertebrates [7–9], yet direct neural correlates of attention are scarce from all animal groups [10]. Here, we demonstrate responses from an identified dragonfly visual neuron [11, 12] that perfectly match a model for competitive selection within limits of neuronal variability ( $r^2 = 0.83$ ). Responses to individual targets moving at different locations within the receptive field differ in both magnitude and time course. However, responses to two simultaneous targets exclusively track those for one target alone rather than any combination of the pair. Irrespective of target size, contrast, or separation, this neuron selects one target from the pair and perfectly preserves the response, regardless of whether the “winner” is the stronger stimulus if presented alone. This neuron is amenable to electrophysiological recordings, providing neuroscientists with a new model system for studying selective attention.

## Results

We recorded intracellularly from the “centrifugal small-target motion detector” neuron CSTMD1 [13], a recently identified binocular neuron from the dragonfly midbrain. It responds selectively to small ( $1^\circ$ – $3^\circ$ ) targets moving across a large receptive field in either excitatory (ipsilateral) or inhibitory (contralateral) visual hemispheres (Figure 1 and see also Figure S1 available online). CSTMD1's neuroanatomy (Figure S1A) is consistent with a possible role in attention as targets move from one visual hemisphere to the other [12, 13]. To test its possible role in the competitive selection of targets, we compared CSTMD1's response to single and paired targets (Figure 1).

Because we cannot instruct a restrained dragonfly to “attend” to one target, we instead use inhomogeneity in the receptive field to determine which of two alternative targets the neuron tracks. When we stimulate CSTMD1 by drifting a small dark target at different locations across a bright LCD screen, differences in the response time course reflect

local inhomogeneity in the receptive field (i.e., variable excitatory and inhibitory synaptic inputs and local differences in spatiotemporal response tuning). Responses are strongest near a frontal “hot spot”  $60^\circ$  above the horizon but also depend on stimulus contrast and size (Figures 1C, 1E, and S1C). This is due in part to the optics of the eye, with a pronounced region of maximal acuity ( $<0.5^\circ$ ) in the frontal-dorsal visual field, falling 3-fold by  $40^\circ$  away [14]. The neuron is correspondingly more sensitive to small targets frontally and larger targets in the periphery (Figure S1C). Although CSTMD1 responds to targets of contrast below 25% (Figure 1E), the receptive field is smaller than for higher contrasts (Figure 1C), with significant responses only in the vicinity of the hot spot.

Receptive fields are similar in the same neuron in different dragonflies. They are also stable over prolonged recording periods, illustrated by the similarity in maps obtained by repeated stimulation of the ipsilateral receptive field (Figures 1B and 1D) and eight identical scans through the hot spot over 15 hr (Figure 1F). Consequently, successive scans of identical targets are very strongly correlated with one another irrespective of their size, contrast, or location ( $r^2 = 0.76$ ) (Figure S2).

The reproducible and unique time-varying response to single targets thus provides a characteristic temporal “fingerprint” that allows us to test our hypothesis: if the neuron selects one target, the response to two simultaneous targets should resemble either one presented alone, not a blend, such as their sum or average. We tested this on unique trajectories  $T_1$  and  $T_2$  (Figure 1B), with either a single target, presented along each trajectory, or both targets presented together (“Pair”).  $T_1$  alone yields a strong response to  $2.5^\circ$ , high-contrast targets (a near-optimal stimulus frontally) shortly after onset and passes through the hot spot, giving a maximal response late in the time course (Figure 1G). The more peripheral  $T_2$  yields a response that increases more gradually before declining (at least for the neuron shown in Figure 1H). The time course depends also on the target size or contrast selected: smaller or lower-contrast targets yield weaker overall responses.

Our primary result is illustrated in Figure 2 by the Pair responses, which consistently resemble the responses for one or the other single target. In Figure 2A,  $T_1$  (red) and  $T_2$  (blue) were small ( $1.25^\circ$  square) targets  $20^\circ$  apart. After an initial lag in which the Pair response (black) is weaker than either single target, it closely follows the temporal fingerprint for  $T_1$  alone. Figures 2B and 2C show examples from two further neurons (N2 and N3 in Figure 2) for targets that are both small ( $1.25^\circ$ ) and low contrast. In both neurons, individual target responses are delayed, eventually responding robustly near the hot spot. Receptive field asymmetry delays the  $T_2$  response more than  $T_1$  (Figure 1C). Intriguingly, when we present the Pair stimulus, the response appears to “lock” onto the  $T_1$  fingerprint, even after  $T_1$  passes out of the receptive field on that trajectory. The response falls to baseline levels, even though  $T_2$  is still within the receptive field. The Pair response thus appears to encode a single selected stimulus and ignore the other.

\*Correspondence: [steven.wiederman@adelaide.edu.au](mailto:steven.wiederman@adelaide.edu.au) (S.D.W.), [david.ocarroll@adelaide.edu.au](mailto:david.ocarroll@adelaide.edu.au) (D.C.O.)

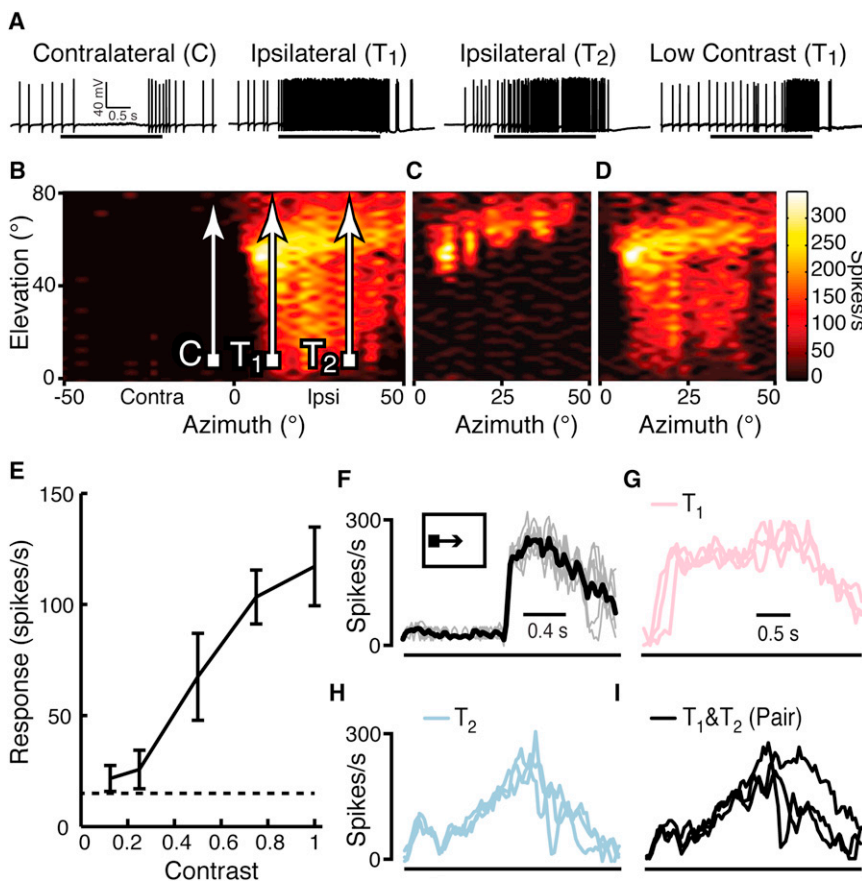


Figure 1. Receptive Fields of CSTMD1 in *Hemiscordulia tau* and Response to Moving Targets (A) Dark targets drifted vertically ( $42^\circ/s$ ) on a white background ( $315 \text{ cd/m}^2$ ,  $120 \text{ Hz}$  LCD display) within the contralateral field suppress intracellular responses to below spontaneous levels. Identical targets moved in the ipsilateral hemifield ( $T_1$ ,  $T_2$ ) evoke excitatory responses with strength dependent on stimulus contrast (high = 1, low =  $0.56$ ,  $I_{\text{difference}}/I_{\text{background}}$ ). (B) Target 1 ( $T_1$ ) moves through the receptive field hot spot and Target 2 ( $T_2$ ) is located  $20^\circ$  to the right. (C) A lower-contrast target maps a smaller receptive field. (D) Receptive field remapped as in (B), revealing consistent inhomogeneity in spatial structure. (E) CSTMD1 (“centrifugal small-target motion detector” neuron) responses to targets of varying contrast drifted horizontally through the receptive field hot spot (mean  $\pm$  SEM,  $n = 8$  neurons, dashed line = mean spontaneous rate). (F) Eight target scans over a 15 hr period reveal low neuronal variability (gray lines: individual responses; black line: mean). (G) CSTMD1 response to three trials of the single  $T_1$  stimulus (red), (H) single  $T_2$  (blue), or (I) simultaneous presentation of both  $T_1$  and  $T_2$  (“Pair” black).

In two of three further trials from N2 with larger targets ( $2.5^\circ$ ), the Pair response follows  $T_2$ , despite this being weaker than  $T_1$  (Figures 2D and 2E). In the third trial, the response is initially identical but “switches” midway to closely track the stronger  $T_1$  (Figure 2F). In a further trial with smaller targets ( $1.25^\circ$ ) and two trials using lower contrasts, we see the opposite result: Pair now resembles the initially stronger  $T_1$  until midway, before switching to  $T_2$  (Figures 2G–2I). Although this switching behavior is not seen in every trial, most examples occur when responses to individual targets are equally strong, suggestive of an underlying competitive mechanism. With near-optimal stimuli ( $2.5^\circ$  targets, high contrast) (Figures 2J–2L), both  $T_1$  and  $T_2$  yield very strong initial responses ( $>250$  spikes per second), a characteristic typically shared by Pair (e.g., Figure 2J). Rarely, however, there is a pronounced delay before Pair closely tracks an individual target (e.g., Figures 2K and 2L), further suggesting initial competitive interactions.

We tested stimuli, as illustrated by Figure 2, across varied combinations of size, contrast, or separation of target pairs. Individually, these produce radically different response time courses for  $T_1$  and  $T_2$ . The Pair response, however, consistently appears to select one target. Nevertheless, selection is somewhat independent of the potency of a stimulus, at least as evidenced by the receptive field of CSTMD1. The selected target can be either  $T_1$  or  $T_2$ , regardless of which one causes stronger CSTMD1 responses (Figure S3A). This variation in target choice suggests that selection involves a process akin to selective attention in vertebrates, a “cognitive” filter to focus on one particular target even in the presence of an equally (or more) salient distracter [15–17].

Could the qualitative match between Pair and  $T_1$  or  $T_2$  be a chance observation resulting from neuronal variability? Figure 3 shows scatter plots (color saturation indicates the density of multiple points; 25 ms bins) for responses within the receptive field from 72 trials at  $20^\circ$  separation, pooled across all four combinations of target size and contrast, over nine neurons. We see a weak correlation when we plot responses for Pair against either  $T_1$  ( $r^2 = 0.58$ ) or  $T_2$  ( $r^2 = 0.35$ ) (Figures 3A and 3B). This confirms that the response to the Pair stimulus does not simply reflect the response to  $T_1$  or  $T_2$  alone. However, if we assume that competitive selection operates to track either target at a given time point, by plotting Pair against either  $T_1$  or  $T_2$ , after computing whichever provides the least difference, we see a very strong correlation ( $r^2 = 0.83$ ) (Figure 3C). Were  $T_1$  and  $T_2$  similar to one another, some improvement in this correlation might be expected from neuronal variability, because this analysis compares Pair with two possible alternatives at each time point. Our deliberate selection of different trajectories for  $T_1$  and  $T_2$ , however, ensures that this is rarely the case, evidenced by both the raw data (Figure 2) and the much weaker correlation of  $T_1$  with  $T_2$  ( $r^2 = 0.27$ ) (Figure 3D). Indeed, the assumption of competitive selection yields a correlation as strong as for subsequent repetitions of identical trials at  $T_1$  or  $T_2$  mean ( $r^2 = 0.76$ ) (Figure S2). We conclude that, within limits of neuronal variability, the Pair response is usually identical to that for one of the targets presented alone.

We can further quantify whether Pair responses reflect competitive selection by considering differences between Pair and alternative combinations of  $T_1$  and  $T_2$ . Figure 4A shows an example model for hypothetically “perfect” competitive selection based on the actual values of  $T_1$  or  $T_2$  responses that correspond most closely to the Pair response. The close match between this model and the observed Pair response

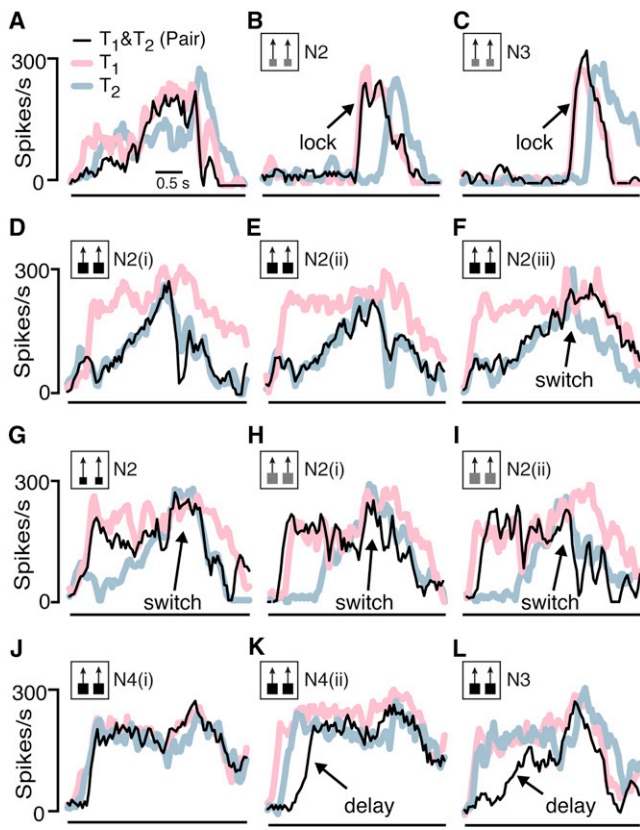


Figure 2. Instantaneous Spike Rate Plots from Single Trials in Four Different CSTMD1 Neuron Recordings, Using a Variety of Sizes and Contrasts

Targets were presented either individually along the trajectories shown in Figure 1B ( $T_1$ , red lines;  $T_2$ , blue lines) or as a Pair stimulus along both trajectories simultaneously (black lines).

(A) Pair response of neuron 1 ( $N_1$ , the same neuron as in Figures 1A–1D) to high-contrast large targets ( $2.5^\circ$ ) is initially weaker than either  $T_1$  or  $T_2$ , before closely tracking  $T_1$  presented alone.

(B and C) Recordings from two neurons ( $N_2$ ,  $N_3$ ) using smaller ( $1.25^\circ$  square), low-contrast targets. As seen in Figure 1D, the receptive field for this stimulus is smaller and at notably lower elevation for  $T_1$  than  $T_2$  (and thus encountered by  $T_1$  250 ms earlier). Under these conditions, the Pair response typically “locks” on to the earlier  $T_1$  and does not switch to  $T_2$ , even after  $T_1$  leaves the receptive field completely at that location.

(D–F) Three identical repetitions of large ( $2.5^\circ$ ), high-contrast targets presented to neuron  $N_2$ . In the third trial, the Pair response “switches” midway, from  $T_2$  to the response produced by  $T_1$  alone.

(G) Further recording from neuron  $N_2$ , using smaller ( $1.25^\circ$ ) targets than in (B). The Pair response initially follows  $T_1$  before switching to  $T_2$ .

(H and I) similar behavior is shown in response to large ( $2.5^\circ$ ), low-contrast targets.

(J and K) Two identical trials using  $2.5^\circ$ , high-contrast targets in neuron  $N_4$  (i.e., as in D–F). In this neuron, the stimulus evokes potent responses to both  $T_1$  and  $T_2$  in the early part of the time course. In the second trial ( $N_4$ , ii), the neuron response to Pair exhibits an onset “delay” before closely tracking  $T_2$ .

(L) A similar lag in response to Pair in neuron  $N_3$  to the same stimulus.

is evident from consistently small errors (lower plots), compared with the difference between Pair and individual  $T_1$  and  $T_2$  responses. We computed the distribution of such errors across four stimulus combinations (large and small targets, high and low contrast) for this competitive selection model and for several alternative models combining the  $T_1$  and  $T_2$  responses: (1) The average of the observed  $T_1$  and  $T_2$  responses (Figure 4B): we might expect this model to best

predict the Pair response if the observations simply reflected neuronal variability from trial to trial. (2) A model for saturating summation of  $T_1$  and  $T_2$  responses (Figure 4C): we might expect the Pair response to best match this model if the two individual responses simply sum (taking into account the potent response to individual targets and the observation that spike rates saturate at  $\sim 300$  spikes per second). (3) A “maximum” model (Figure 4D) based on the stronger of either the  $T_1$  and  $T_2$  response and (4) the corresponding “minimum” model (not shown): we might expect these models to best predict the Pair response if target selection simply favored the stronger or weaker individual stimulus.

The tightest and most symmetrical error distribution for these model varieties is for competitive selection ( $n = 72$  trials over 9 neurons) (Figures 4E and 4F). Figure 4G shows the linearly weighted sum of signed errors for target pairs with  $20^\circ$  separation (mean  $\pm$  95% confidence index [CI],  $n = 18$ ). Negative errors reflect Pair responses weaker than model predictions and vice versa. Although the four stimulus conditions produce different responses (in both magnitude and time course), as seen in Figure 2, competitive selection consistently provides the best explanation for the activity observed for Pair stimulation, with significantly smaller total errors over all target conditions, compared with every other model (one-way ANOVA, Dunnett’s multiple comparison  $p < 0.001$ ,  $n = 72$ ). The effect size for these comparisons is large (Cohen’s  $d$ , 95% CI): average, 1.3 [0.9, 1.6]; summation, 2.9 [2.5, 3.4]; maximum, 1.7 [1.3, 2.1]; minimum, 1.2 [0.8, 1.5]. Positive bias in errors for the minimum model and negative bias for the maximum model suggests that the Pair response stays tightly bounded by  $T_1$  and  $T_2$ , regardless of which is stronger. This is confirmed by the similarity in the division of time that Pair “tracks”  $T_1$  versus  $T_2$  (Figure S3A). Mainly negative errors for the summation model confirm no additive effect between individual responses, even at large separation (Figure S3B). As we decrease target separation to  $5^\circ$ , larger negative errors (Figure S3B) probably reflect lateral inhibitory interactions between targets at earlier stages of visual processing [13].

## Discussion

Our data make a compelling case that CSTMD1 reflects competitive selection of one target. We emphasize “competitive,” because the attended target is not always the same between trials or even within a trial, as seen in strikingly perfect switches from one to the other (e.g., Figures 2F–2I). Competition is further suggested by rare examples where the activity observed under Pair stimulation initially lags both  $T_1$  and  $T_2$  responses (e.g., Figures 2K and 2L), suggesting initial conflict in the underlying neural network before resolution of competition by a “winning” target. Variability in the actual winner suggests either modulation of the underlying salience of targets over trials (e.g., via local habituation) or a higher-order mechanism of bias [19].

We previously showed that CSTMD1 still responds robustly to a target even when it is embedded within a high-contrast natural scene containing numerous potential distracters [20]. Taken together with recent evidence that the behavioral state of insects strongly modulates responses of neurons involved in visuomotor control [21], our new data thus suggest a hitherto unexpected sophistication in higher-order control of insect visual processing, akin to selective attention in primates. Perhaps the most remarkable feature of our data is that once the response “locks” onto a target (or following a switch),

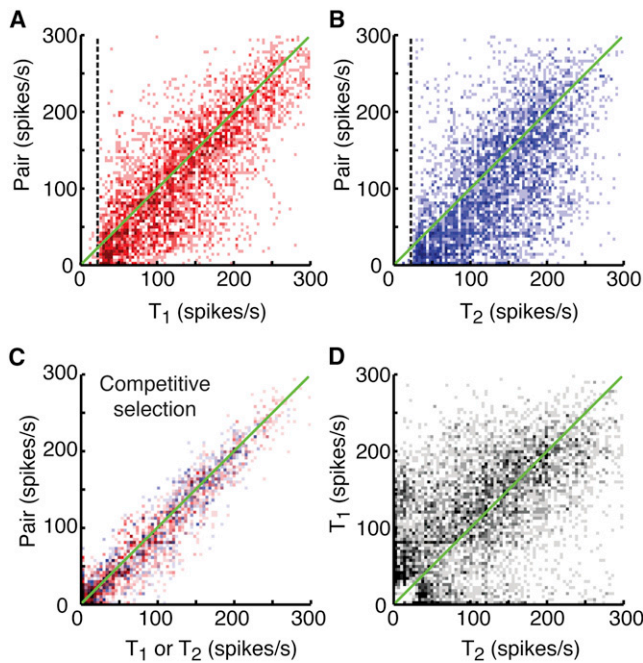


**Figure 3. Correlation Analysis Reveals Competitive Selection Underlies the Paired Response**

Peristimulus time histograms (25 ms bins) were lightly filtered (Savitzky-Golay [18], 2<sup>o</sup>, 7 span). Data for further analysis were taken from bins where stimuli were within the receptive field, determined via an inclusion criterion of T<sub>1</sub> or T<sub>2</sub> above a threshold of 1.5 × SD of the spontaneous activity for each cell.

(A and B) Each time point formed density scatter plots for: (A) Pair versus T<sub>1</sub> ( $r^2 = 0.58$ ) and (B) Pair versus T<sub>2</sub> ( $r^2 = 0.35$ ). There is a stronger association between Pair and T<sub>1</sub>, the trajectory that traverses the receptive field hot spot. Dashed lines show the average inclusion threshold, and the green line is a slope of 1.

(C) We define “competitive selection” as the response of either T<sub>1</sub> (red points) or T<sub>2</sub> (blue points), dependent on which target has the least difference to the Pair response. An  $r^2$  of 0.83 indicates that Pair is highly correlated with either T<sub>1</sub> or T<sub>2</sub> at all times. This value is similar to neuronal variability of a repeated T<sub>1</sub> stimulus ( $r^2 = 0.81$ ) (see Figure S2).

(D) Weak correlation between T<sub>1</sub> and T<sub>2</sub> ( $r^2 = 0.27$ ) confirms inhomogeneity in receptive field structure.

the second target exerts no influence on the neuron’s response: the distracter is ignored completely (Figures 2B and 2C). This highly accurate encoding of single stimuli is in contrast with competitive selection described for neurons in the primate lateral intraparietal area (LIP) [22] and avian midbrain [23, 24]. These tend to represent relative stimulus salience, with responses still modulated by the strength of distracters outside the receptive field. Our results are more similar to data from primate visual cortex, where responses to stimulus pairs within the receptive field comprising both preferred and antipreferred stimuli tend toward responses for the individual stimulus that the animal attends to [3, 25–27].

Accurate encoding of an “attended” target independent of distracters would be invaluable for control of target pursuit, because it would enable prey tracking amidst swarms of distracters, using the exact same gain in the control loop as in a simpler scenario, where the prey is the sole salient target. We have no direct evidence for where CSTMD1 sits within such a control system or indeed for the hierarchy of underlying mechanisms of competitive selection. The invertebrate brain is a highly coupled neuronal network, with efferent circuitry

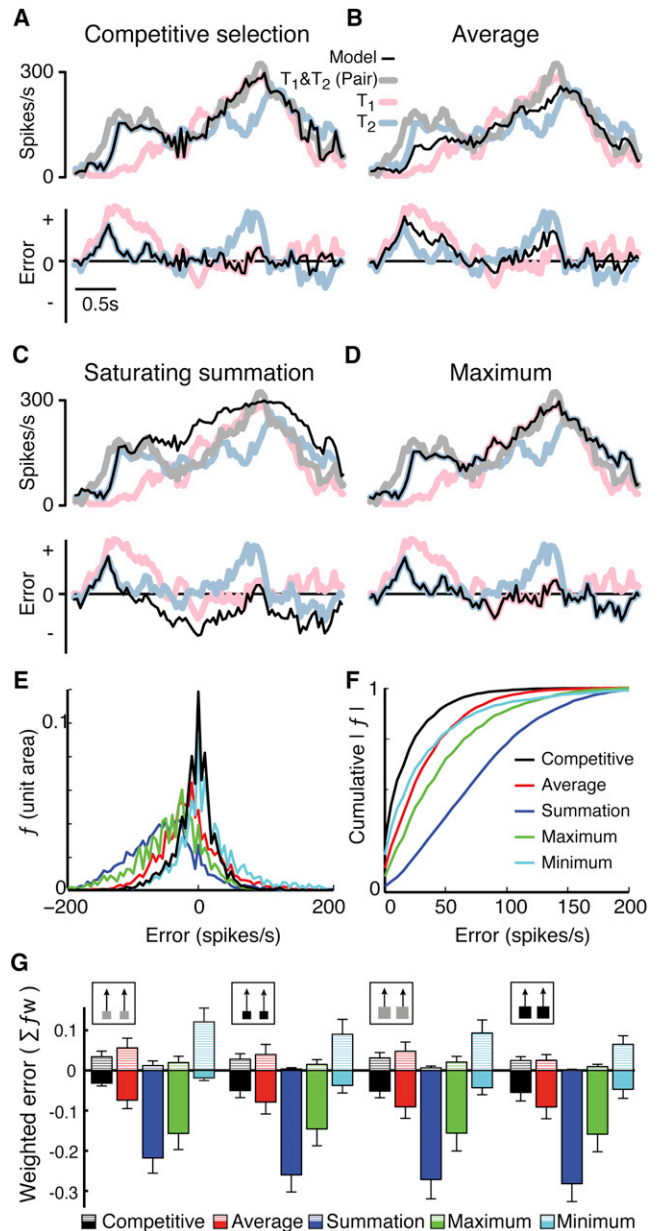


**Figure 4. Competitive Selection More Accurately Matches Paired Responses than Alternative Models**

(A) An example of CSTMD1 response (upper) to T<sub>1</sub> (red), T<sub>2</sub> (blue), or Pair (gray) and a model for competitive selection (black line) based on the actual value of either T<sub>1</sub> or T<sub>2</sub> that most closely resembles Pair. The lower plots show errors between observed Pair and either model (black), T<sub>1</sub> (red), or T<sub>2</sub> (blue). Negative errors represent Pair responses below model predictions.

(B–D) This is the same as for (A) but where the model is: (B) the average of T<sub>1</sub> and T<sub>2</sub>, (C) summation of T<sub>1</sub> and T<sub>2</sub> followed by a saturating nonlinearity (see text), or (D) maximum of T<sub>1</sub> or T<sub>2</sub>.

(E and F) (E) Frequency histograms and (F) cumulative frequency (unsigned) of all errors (normalized to unit area,  $n = 72$ ). The narrowest error distribution is for competitive selection, with 91% of the data within an error less than 50 spikes per second.

(G) Linearly weighted errors (mean ± 95% CI) for the four target conditions. In each, competitive selection matches the Pair response with least errors, centered on zero ( $n = 18$ ).

projecting to even the most distal levels of sensory processing [28]. CSTMD1 itself is a high-order efferent neuron, with its major dendritic input in the midbrain. The axon traverses the brain to contralateral arborizations coincident with the inputs of its mirror symmetric counterpart and a second set of extensive arborizations over the contralateral optic lobe [12, 29]. This morphology, in conjunction with the inhibition by targets presented in the contralateral visual field (Figures 1A and S1B; [13]), suggests a form of interhemispheric gating control by the competitively selected inputs.

It is possible, then, that CSTMD1 reflects the output of exogenous (bottom-up) attention mediated via a competitive process occurring at a lower level in the STMD pathway. However, we cannot rule out the possibility that target selection reflects a top-down, endogenous attention process. We recently showed that CSTMD1's response builds up slowly over hundreds of ms when single targets move along long trajectories [29, 30]. This slow facilitation could represent "arousal," as also observed in locust anticollision neurons [31]. Alternatively, it may resemble enhanced responses in primate visual cortex once attention is directed to a single stimulus [32, 33]. The rare cases where Pair initially lags both T<sub>1</sub> and T<sub>2</sub> responses (e.g., Figures 2K and L) may thus be analogous to recent data from primate area V4, where pattern selectivity for a "sought-after" target builds 40 ms after selectivity for "hard-wired" features, such as color, shape, or orientation [34].

Our finding of a process analogous to selective attention in primates is particularly exciting because insects have proved to be powerful tools for "circuit-busting" neuronal computations in biological motion vision [35], inspiring substantial breakthroughs in computational models with diverse applications [36–38]. Insect preparations are amenable to physiological and pharmacological intervention *in vivo*, with major progress also now being made via selective genetic knock-down, at least in fruit flies [39, 40]. Nevertheless, our experimental preparation offers some disadvantages compared with preparations such as the awake, behaving monkey. Intracellular recordings require immobilization of head movements, preventing our dragonflies from directing gaze toward attended targets (overt attention) during experiments. Such fixation head movements have certainly been observed during free-flight pursuit of prey, using high-speed video techniques [41]. Controlled, endogenous focus on a particular area or feature (selective attention) in primate models functions via interaction with neuronal circuits of reward, memory, and sensory-motor coupling [42–44]—all of which have analogous circuitry in the invertebrate brain [21, 45, 46]. Although we have yet to find a way to train or reward dragonflies for covertly attending to a specific location, we may be able to manipulate the "attended" target more explicitly by carefully controlling the presentation order and initial location of the target and distracters in future experiments.

#### Supplemental Information

Supplemental Information includes three figures and Supplemental Experimental Procedures and can be found with this article online at <http://dx.doi.org/10.1016/j.cub.2012.11.048>.

#### Acknowledgments

This work was supported by the US Air Force Office of Scientific Research (FA2386-10-1-4114). We thank the manager of the Botanic Gardens in Adelaide for allowing insect collection.

Received: October 9, 2012

Revised: November 8, 2012

Accepted: November 26, 2012

Published: December 20, 2012

#### References

1. Corbet, P.S. (1999). *Dragonflies: Behavior and Ecology of Odonata* (Ithaca, NY: Cornell University Press).
2. Kastner, S., De Weerd, P., Desimone, R., and Ungerleider, L.G. (1998). Mechanisms of directed attention in the human extrastriate cortex as revealed by functional MRI. *Science* 282, 108–111.
3. Moran, J., and Desimone, R. (1985). Selective attention gates visual processing in the extrastriate cortex. *Science* 229, 782–784.
4. Desimone, R., and Duncan, J. (1995). Neural mechanisms of selective visual attention. *Annu. Rev. Neurosci.* 18, 193–222.
5. McPeck, R.M., and Keller, E.L. (2004). Deficits in saccade target selection after inactivation of superior colliculus. *Nat. Neurosci.* 7, 757–763.
6. Tsotsos, J.K., Culhane, S.M., Wai, W.Y.K., Lai, Y., Davis, N., and Nuflo, F. (1995). Modeling visual attention via selective tuning. *Artif. Intell.* 78, 507–545.
7. Pollack, G.S. (1988). Selective attention in an insect auditory neuron. *J. Neurosci.* 8, 2635–2639.
8. Greenspan, R.J., and van Swinderen, B. (2004). Cognitive consonance: complex brain functions in the fruit fly and its relatives. *Trends Neurosci.* 27, 707–711.
9. van Swinderen, B. (2007). Attention-like processes in *Drosophila* require short-term memory genes. *Science* 315, 1590–1593.
10. Knudsen, E.I. (2007). Fundamental components of attention. *Annu. Rev. Neurosci.* 30, 57–78.
11. O'Carroll, D. (1993). Feature-detecting neurons in dragonflies. *Nature* 362, 541–543.
12. Geurten, B.R.H., Nordström, K., Sprayberry, J.D.H., Bolzon, D.M., and O'Carroll, D.C. (2007). Neural mechanisms underlying target detection in a dragonfly centrifugal neuron. *J. Exp. Biol.* 210, 3277–3284.
13. Bolzon, D.M., Nordström, K., and O'Carroll, D.C. (2009). Local and large-range inhibition in feature detection. *J. Neurosci.* 29, 14143–14150.
14. Horridge, G.A. (1978). The separation of visual axes in apposition compound eyes. *Philos. Trans. R. Soc. Lond. B Biol. Sci.* 285, 1–59.
15. Broadbent, D.E. (1958). *Perception and Communication* (New York: Pergamon Press).
16. Treisman, A.M. (1964). Selective attention in man. *Br. Med. Bull.* 20, 12–16.
17. Posner, M.I. (1980). Orienting of attention. *Q. J. Exp. Psychol.* 32, 3–25.
18. Savitzky, A., and Golay, M.J.E. (1964). Smoothing and differentiation of data by simplified least squares procedures. *Anal. Chem.* 36, 1627–1639.
19. Desimone, R. (1998). Visual attention mediated by biased competition in extrastriate visual cortex. *Philos. Trans. R. Soc. Lond. B Biol. Sci.* 353, 1245–1255.
20. Wiederman, S.D., and O'Carroll, D.C. (2011). Discrimination of features in natural scenes by a dragonfly neuron. *J. Neurosci.* 31, 7141–7144.
21. Maimon, G., Straw, A.D., and Dickinson, M.H. (2010). Active flight increases the gain of visual motion processing in *Drosophila*. *Nat. Neurosci.* 13, 393–399.
22. Bisley, J.W., and Goldberg, M.E. (2003). Neuronal activity in the lateral intraparietal area and spatial attention. *Science* 299, 81–86.
23. Asadollahi, A., Mysore, S.P., and Knudsen, E.I. (2010). Stimulus-driven competition in a cholinergic midbrain nucleus. *Nat. Neurosci.* 13, 889–895.
24. Mysore, S.P., Asadollahi, A., and Knudsen, E.I. (2011). Signaling of the strongest stimulus in the owl optic tectum. *J. Neurosci.* 31, 5186–5196.
25. Treue, S., and Maunsell, J.H. (1996). Attentional modulation of visual motion processing in cortical areas MT and MST. *Nature* 382, 539–541.
26. Reynolds, J.H., Chelazzi, L., and Desimone, R. (1999). Competitive mechanisms subserve attention in macaque areas V2 and V4. *J. Neurosci.* 19, 1736–1753.
27. Lee, J., and Maunsell, J.H.R. (2010). Attentional modulation of MT neurons with single or multiple stimuli in their receptive fields. *J. Neurosci.* 30, 3058–3066.
28. Strausfeld, N.J. (1976). *Atlas of an Insect Brain* (New York: Springer-Verlag).

29. Dunbier, J.R., Wiederman, S.D., Shoemaker, P.A., and O'Carroll, D.C. (2012). Facilitation of dragonfly target-detecting neurons by slow moving features on continuous paths. *Front. Neural Circuits* 6, 79.
30. Nordström, K., Bolzon, D.M., and O'Carroll, D.C. (2011). Spatial facilitation by a high-performance dragonfly target-detecting neuron. *Biol. Lett.* 7, 588–592.
31. Rind, F.C., Santer, R.D., and Wright, G.A. (2008). Arousal facilitates collision avoidance mediated by a looming sensitive visual neuron in a flying locust. *J. Neurophysiol.* 100, 670–680.
32. McAdams, C.J., and Maunsell, J.H. (1999). Effects of attention on orientation-tuning functions of single neurons in macaque cortical area V4. *J. Neurosci.* 19, 431–441.
33. Treue, S., and Martínez Trujillo, J.C. (1999). Feature-based attention influences motion processing gain in macaque visual cortex. *Nature* 399, 575–579.
34. Ipata, A.E., Gee, A.L., and Goldberg, M.E. (2012). Feature attention evokes task-specific pattern selectivity in V4 neurons. *Proc. Natl. Acad. Sci. USA* 109, 16778–16785.
35. Borst, A., and Euler, T. (2011). Seeing things in motion: models, circuits, and mechanisms. *Neuron* 71, 974–994.
36. Franceschini, N., Pichon, J.M., Blanes, C., and Brady, J.M. (1992). From insect vision to robot vision. *Philos. Trans. R. Soc. Lond. B Biol. Sci.* 337, 283–294.
37. Srinivasan, M.V., Chahl, J.S., Weber, K., Venkatesh, S., Nagle, M.G., and Zhang, S.W. (1999). Robot navigation inspired by principles of insect vision. *Robot. Auton. Syst.* 26, 203–216.
38. Wiederman, S.D., Shoemaker, P.A., and O'Carroll, D.C. (2008). A model for the detection of moving targets in visual clutter inspired by insect physiology. *PLoS ONE* 3, e2784.
39. Rister, J., Pauls, D., Schnell, B., Ting, C.Y., Lee, C.H., Sinakevitch, I., Morante, J., Strausfeld, N.J., Ito, K., and Heisenberg, M. (2007). Dissection of the peripheral motion channel in the visual system of *Drosophila melanogaster*. *Neuron* 56, 155–170.
40. Joesch, M., Schnell, B., Raghu, S.V., Reiff, D.F., and Borst, A. (2010). ON and OFF pathways in *Drosophila* motion vision. *Nature* 468, 300–304.
41. Olberg, R.M., Seaman, R.C., Coats, M.I., and Henry, A.F. (2007). Eye movements and target fixation during dragonfly prey-interception flights. *J. Comp. Physiol. A Neuroethol. Sens. Neural Behav. Physiol.* 193, 685–693.
42. Rizzolatti, G. (1983). Mechanisms of selective attention in mammals. In *Advances in Vertebrate Neuroethology*, J.P. Ewart, R.R. Capranica, and D.J. Ingle, eds. (New York: Plenum), pp. 261–297.
43. Maunsell, J.H.R. (2004). Neuronal representations of cognitive state: reward or attention? *Trends Cogn. Sci.* 8, 261–265.
44. Desimone, R. (1996). Neural mechanisms for visual memory and their role in attention. *Proc. Natl. Acad. Sci. USA* 93, 13494–13499.
45. Menzel, R., and Müller, U. (1996). Learning and memory in honeybees: from behavior to neural substrates. *Annu. Rev. Neurosci.* 19, 379–404.
46. Wustmann, G., Rein, K., Wolf, R., and Heisenberg, M. (1996). A new paradigm for operant conditioning of *Drosophila melanogaster*. *J. Comp. Physiol. A Neuroethol. Sens. Neural Behav. Physiol.* 179, 429–436.